**Proceedings of the ASME 2018 International Design Engineering Technical Conferences & Computers and Information in Engineering Conference**
**IDETC/CIE 2018**
**August 26-29, 2018, Quebec City, Canada**

**DETC2018-85640**

# SPIRAL PULLEY NEGATIVE STIFFNESS MECHANISM FOR MORPHING AIRCRAFT ACTUATION

**Jiaying Zhang**[*], **Alexander D. Shaw**
**Mohammadreza Amoozgar**, **Michael I. Friswell**
College of Engineering
Swansea University
Swansea SA2 8PP
United Kingdom

**Benjamin K.S. Woods**
Faculty of Engineering
Department of Aerospace Engineering
University of Bristol
Bristol BS8 1TR
United Kingdom

## ABSTRACT

*The energy balancing concept seeks to reduce actuation requirements for a morphing structure by strategically locating negative stiffness devices to tailor the required deployment forces and moments. One such device is the spiral pulley negative stiffness mechanism. This uses a cable connected with a pre-tension spring to covert decreasing spring force into increasing balanced torque. The kinematics of the spiral pulley are firstly developed and its geometry is then optimised by employing an energy conversion efficiency function. The performance of the optimised spiral pulley is then evaluated through the net torque, the total required energy and energy conversion efficiency. An experiment demonstrates the negative stiffness property of the mechanism and compares its characteristics with the analytical result. Exploiting the negative stiffness mechanism has a significant interest in not only the field of morphing aircraft but many other power reduction applications.an increasing output torque. The kinematics of the spiral pulley are firstly developed and its geometry is then optimised by employing an energy conversion efficiency function. The performance of the optimised spiral pulley is then evaluated through the net torque, the total required energy and energy conversion efficiency. An experiment demonstrates the negative stiffness property of the mechanism and compares its characteristics with the analytical result. Exploiting the negative stiffness mechanism has a significant interest in not only the field of morphing aircraft but also many other energy and power reduction applications.*

## INTRODUCTION

Traditional aircraft structures are designed as a fixed geometry, with actuated substructures connected with discrete mechanical elements such as pinned joints and sliding rails. These designs can add significant mass and adversely influence the flight performance and energy consumption at the aircraft system level. Morphing aircraft seek to remedy this by integrating actuation into the structures themselves, and this is receiving widespread interest across the aerospace industry, because the flight performance and energy efficiency can be improved [1–5].

Many approaches to actuation have been applied to morphing aircraft; piezoelectric materials have been used as actuators for control surfaces [6], spanwise deflection [7] and trailing-edge flaps [8, 9]. Meanwhile, other smart materials, such as shape memory alloys, have been investigated for morphing structures [10–13]. Moreover, the multistable characteristics of some special structures may be designed as substructures to achieve continuous morphing. A series of bistable prestressed buckled laminates has been arranged to construct a bistable rotor blade flap, which is actuated by a matched actuator [14]. The morphing of an aircraft wing in the chord direction has also been investigated by employing an array of bistable arches, which can

[*]Address all correspondence to this author (jiaying.zhang@swansea.ac.uk).

be actuated to accomplish chord extension [15]. Although these different methods have been verified to provide the possibility for morphing aircraft, the actuating energy required is dependent on external actuators, which can have a significant negative impact on system level performance due to added mass and energy requirements. Therefore, minimising this external energy input can be key to optimising morphing aircraft at the system level.

The objective of this paper is to develop an energy balancing system for morphing aircraft. The key component of this objective is using an additional negative stiffness system to balance the positive stiffness of the morphing system, therefore reducing actuation effort. Although the concept of using negative stiffness systems has been generally used to achieve stiffness changes in a dynamic system [16, 17], the alternative use of negative stiffness systems can be beneficial for statically balanced, especially for morphing aircraft. An energy balancing adjustment system has been developed for gravity equilibrators, which use extended springs to supply or store the necessary energy and the rotation of a fixed geometry bar to produce static balance [18]. Moreover, spring-pulley systems have been developed previously, for instance, a cam based balancers with the varying radius pulley can preserve moment equilibrium between a constant load and a varying spring length [19, 20]. Previous works have been undertaken by Woods, Friswell and Wereley, where a pneumatic actuator was used to provide the driving force, and a spiral shaped pulley was used to provide kinematic tailoring [21]. The output load line of the actuator was modified to match an assumed torque for driving a compliant morphing aircraft. Then, an extension spring based system was set up to investigate this concept further [22].

This work extends [22] by considering the application to a specific design target taken from a relevant morphing aircraft application which is different to the previous work on the concept that looked only at balancing a completely arbitrary stiffness (1000 N/m). In order to investigate how to setup an energy balancing system, a spiral pulley negative stiffness mechanism is developed to balance the positive stiffness required to deform a camber morphing aerofoil based on the Fish Bone Active Camber (FishBAC) concept. Energy is used here as an index to show the contribution of reducing the required actuation input by using such negative stiffness mechanism. Firstly, the FishBAC wing section is chosen as the target morphing structure, and the required torque in real conditions is presented. Then, in order to obtain a suitable geometry of the spiral pulley, an energy conversion efficiency function is derived as an objective for optimisation. Through minimisation of the energy conversion efficiency function, an applicable spiral pulley negative stiffness mechanism can be obtained with satisfactory energy index, which matches the torque required closely. The results of the analysis are then confirmed experimentally.

## Morphing aircraft actuation

In order to investigate how to use a negative stiffness mechanism for morphing aircraft actuation, a simple new morphing concept known as the Fish Bone Active Camber (FishBAC) [23] is chosen as the drive load for study. This concept uses a biologically inspired internal bending beam and elastomeric matrix composite as skin surface, as shown in Fig. 1 [23]. The benefit of this concept is that it is capable of large camber changes and morphing the camber of an airfoil smoothly and continuously. The rotation of the tendon spooling pulley tensions the tendons to morph the trailing edge upward or downward and produces a continuous change of the camber.

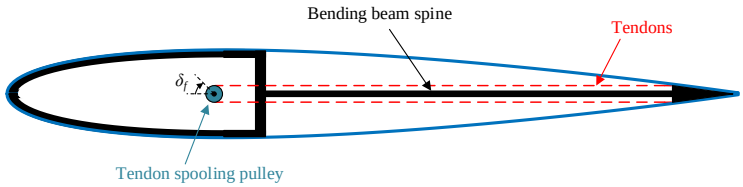


**FIGURE 1**. Schematic of FishBAC concept [23].

For this study, the target operating range of the FishBAC and the corresponding aerodynamic performance and actuation requirements were generated using a previously developed fluid-structure interaction (FSI) analysis [24, 25]. This FSI analysis couples a low-fidelity analytical representation of the FishBAC structure to the XFOIL viscous panel method, and also includes consideration of elasticity in the drive tendons. Figure 2 shows that FishBAC camber is predicted to generate a maximum lift coefficient of $C_l = 1.46$ when fully deflected, which can produce a vertical trailing-edge displacement of $w_e$ = 14mm (5.2% of chord) and a tendon pulley rotation of $\delta_f$ = 60 deg, as shown in Fig. 3 .

Figure. 4 shows that the compliant FishBAC camber can be considered as a positive stiffness system, and the required torque is proportional to the rotation angle. Therefore, the required torque for morphing will be linearised to produce a target positive stiffness system for designing the spiral pulley negative stiffness mechanism in the following research. This positive stiffness system requires energy input in order to deform, and currently this energy is not recovered upon return to the undeformed case. Indeed, most morphing aircraft concepts require energy input to morph, and very few of them are able to recover that energy to any meaningful degree. This then provides the fundamental underlying motivation for this work. The negative stiffness device proposed here is essentially an energy storage device, as the energy required to overcome the positive stiffness

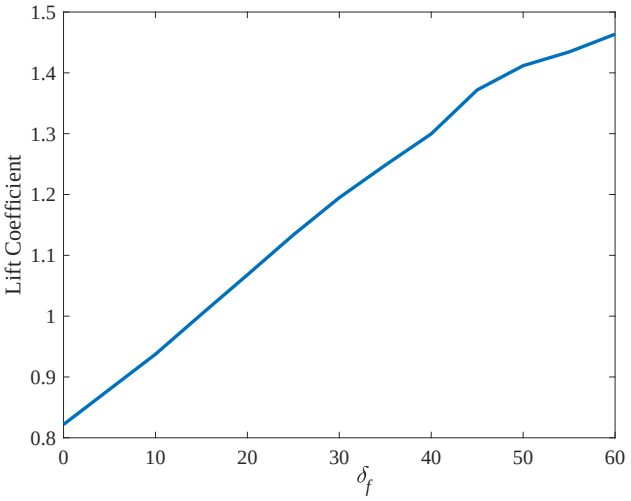


**FIGURE 2**. Lift coefficient of the different morphing rotation.

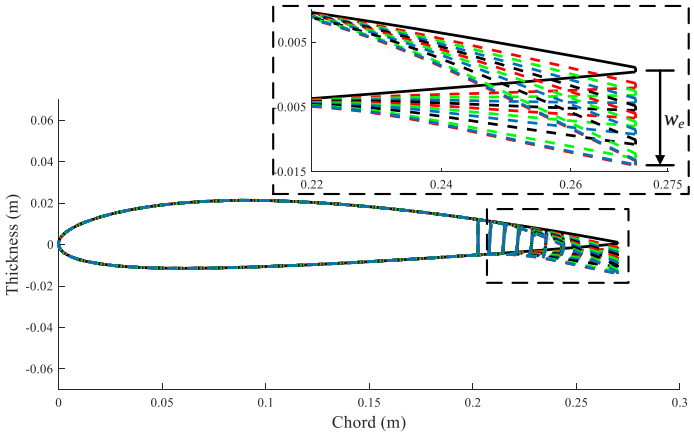


**FIGURE 3**. Objective of morphing the FishBAC model.

of the morphing device is provided by it, and is then returned to it as the morphing device returns to its undeformed state. The effect of this passive approach to balancing the energy required is that the actuation effort (in terms of both torque and energy) is significantly reduced by using stored energy to achieve passive energy balancing. These two systems will be combined together so that they can cancel each other to produce a near-zero stiffness system. This is valuable for morphing structures where the structures support significant loads during frequent actuation.

The chosen negative stiffness mechanism is a spiral pulley negatives stiffness device, as shown in Fig. 5. A linear spring is used here to store energy and produce actuating force. As the spiral pulley rotates, its effective diameter changes, and the moment arm produced by the profile of the spiral pulley varies. This

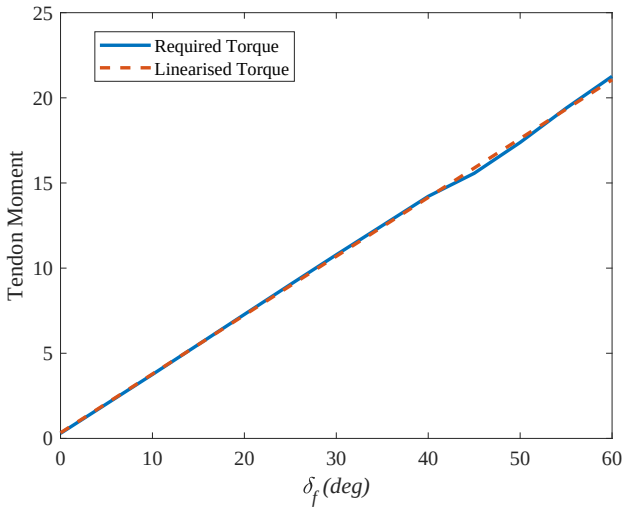


**FIGURE 4**. Comparison of required torque and the corresponding linearised torque.

effect can be tailored to give negative stiffness, and optimised for a given actuation role. In addition, this work is considering to apply the spiral pulley negative stiffness mechanism for morphing aircraft actuation, some more practical situations should be considered. It can be easily understood that the required actuation effort will increase as the required morphing deflections and effort increase. It is hard to satisfy both the actuation requirement and the limited space to develop an energy balancing system for large morphing aircraft requirements. Therefore, in order to explore the possibilities for improvement of the integrated performance, a gear is proposed as an additional parameter to produce a larger tolerances for reducing dimension of the system. The benefit of using the gear provides a possibility to design a smaller spiral pulley negative stiffness mechanism by modifying the gear ratio ($G$) between the input and output. The schematic of the whole system is shown in Fig. 5, from an initial configuration to an actuated configuration.

## Spiral pulley negative stiffness mechanism

The analysis of a passively energy balanced FishBAC morphing airfoil employing the spiral pulley negative stiffness concept, which is shown schematically in Fig. 5, is presented here. The complicated kinematics of the spiral pulley and spooling cable are first investigated, as shown in Fig. 5. Then, an energy conversion efficiency based objective function is proposed and the nonlinear programming solver *fmincon* is used to optimise the objective function.

Although any profile of the pulley can be used to produce variation in radius, an exponential radius function was chosen

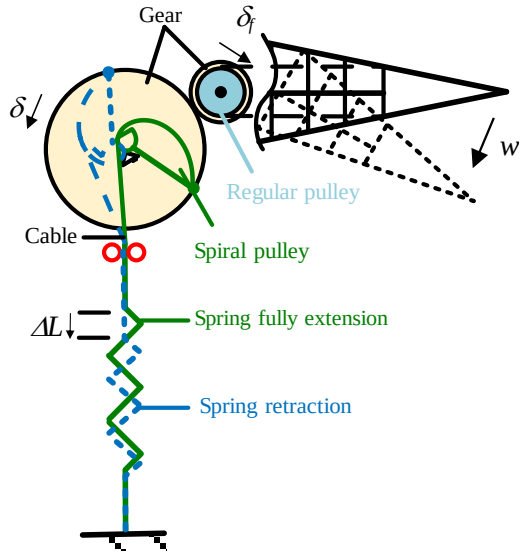


**FIGURE 5**. Schematic of spiral pulley negative stiffness mechanism for morphing aircraft actuation.

as potentially the best match to the desired nonlinear force profile. The detailed geometry definition of the spiral pulley is then shown in Fig. 6. The spiral pulley is firstly defined as an exponential radius profile in polar coordinates about the centre of rotation $O$

$$r = r_0 + k_1 e^{k_2(\theta+\delta+\delta_f)} \tag{1}$$

where $\delta$ is spiral pulley rotation angle and $\theta$ is a parameter associated with it; $\delta_0$ is initial pulley rotation angle; $r_0$, $k_1$and $k_2$ are parameters of the spiral profile, respectively. A wide range of different radius profiles can be used for the spiral pulley, with different shape functions being better suited to different load profiles. The exponential function used here has been shown to be well suited to the linear stiffness we wish to balance in this case [22].

Figure 6 shows that the cable is wrapped around the spiral pulley and point $B$ is the initial point of contact. The Cartesian coordinates can then be defined with the origin point at $A$ and the coordinates of any point $B$ can then be defined as

$$x_B = x_{off} - r\sin\theta \tag{2}$$

$$y_B = y_{off} - r\cos\theta \tag{3}$$

Therefore, the length of the vector $\overline{OA}$ is equal to

$$l_{off} = \sqrt{x_{off}^2 + y_{off}^2} \tag{4}$$

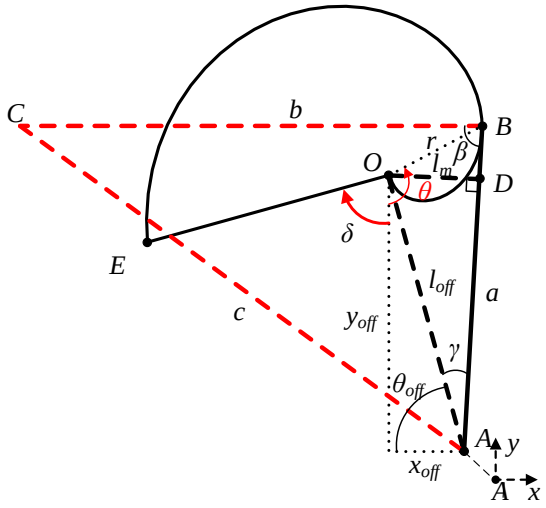


**FIGURE 6**. Spiral pulley geometry analysis with moment arm details.

In addition, length of the cable between the origin point $A$ and point $B$ is equal to

$$a = \sqrt{x_B^2 + y_B^2} \tag{5}$$

As mentioned above the cable is wrapped around the spiral pulley from point $B$ to the cable anchor point $E$. The arc length of the wrapped cable is then obtained as

$$\begin{aligned} S &= \int_{\theta(B)}^{\theta(E)} \sqrt{r^2 + (\frac{dr}{d\theta})^2} d\theta \\ &= \int_{\theta(B)}^{\theta(E)} \sqrt{(r_0 + k_1 e^{k_2(\theta+\delta)})^2 + (k_2 k_1 e^{k_2(\theta+\delta)})^2} \end{aligned} \tag{6}$$

Therefore, the total length of the cable from point $A$ to point $E$ is equal to

$$L = b + S \tag{7}$$

Since the length of the cable between spiral pulley and extension spring is essentially constant, as shown in Fig. 5, the rotation of the spiral pulley leads to the release of a portion of the cable. The change in the spring length can be calculated by subtracting the total cable length evaluated at each spiral pulley rotation angle $\delta$, from the total cable length at the initial pulley rotation angle $\delta_3$.

$$\Delta L = L_\delta - L_{\delta_0} \tag{8}$$

Then, the moment produced by the force in the cable varies due to the change of the moment arm $\overline{OD}$, which is defined as $l_m$, the length of the vector perpendicular to the straight cable $\overline{AB}$. In order to calculate the length $l_m$, it is necessary to add an additional guide $\overline{BC}$ with an arbitrary fixed length of $\overline{BC} = b$ and parallel to the horizontal axis. The coordinates of point $C$ can then be determined as

$$x_C = x_B - b \tag{9}$$

$$y_C = y_B \tag{10}$$

$b$ is taken to be 50 mm for analysis here. The length of vector $\overline{AC}$ is equal to

$$C = \sqrt{x_c^2 + y_c^2} \tag{11}$$

The angle $\beta$ can be obtained by using the law of cosines with the known $a$, b and $c$, which is

$$\beta = \cos^{-1}\left[\frac{a^2 + b^2 - c^2}{2ab}\right] \tag{12}$$

The angle of the pulley rotation point relative to the origin $\theta_{off}$ is

$$\theta_{off} = \tan^{-1}(\frac{x_{off}}{y_{off}}) \tag{13}$$

The moment arm angle $\gamma$ in Fig. 3 can therefore be derived by given $\beta$ and $\theta_{off}$

$$\gamma = \pi - \beta - \theta_{off} \tag{14}$$

The length $l_m$ of the moment arm $\overline{OD}$ can finally be solved by Eq. (4) and Eq. (14)

$$l_m = l_{off} \sin\gamma = \sqrt{x_{off}^2 + y_{off}^2} \sin\gamma \tag{15}$$

It is obvious that the above analysis is derived for any point $B$ on the profile of the spiral pulley. Therefore, in order to match the practical situation, it is important to confirm the unique position of point $B$ for each rotation angle $\delta$. In other words, extra conditions should be considered to find the point of tangency between the straight portion of the cable $\overline{AB}$ and the spiral pulley surface. From the viewpoint of the geometry shown in Fig. 3, the point of tangency occurs when point has the minimum corresponding angle $\beta$. Meanwhile, the value of angle $\gamma$ could be considered as a function of variable $\theta$, and the minimum corresponding angle $\beta$ can therefore be solved by differentiating Eq. (12) with respect to $\theta$ and setting the result equal to $\theta$. Thus

$$\left.\frac{d\beta}{d\theta}\right|_{min\beta} = 0 \tag{16}$$

The spring is designed as an energy storage device with an initial length $L_0$ as mentioned above. The force $F_s$ in the spring at the current position can therefore be obtained as

$$F_s = K(L_0 - \Delta L) \tag{17}$$

where $K$ is the spring constant, and the initial tension that exists in practical tension springs will be further discussed. Finally, the torque produced by the spiral pulley can then obtained from Eq. (8) and Eq. (15) for each rotation angle $\delta$, as

$$T_s = F_s l_m \tag{18}$$

Since these two independent systems are connected by a gear, the torque $T_f$ on the FishBAC tendon spooling pulley has to be modified by the gear ratio $G$, to give

$$T_f = T_s G = F_s l_m G \tag{19}$$

The corresponding rotation of the FishBAC tendon spooling pulley is also modified as

$$\delta_f = \frac{\delta}{G} \tag{20}$$

In order to optimise the performance of the energy balancing system, an objective energy conversion efficiency function is proposed to make the torque provided by the spiral pulley system match the required torque as closely as possible. To accomplished this, an energy conversion efficiency metric is defined as

$$\eta_{ef} = \frac{E_o}{E_r} \tag{21}$$

where $E_o$ is the output energy provided from the spiral pulley negative stiffness mechanism,

$$E_o = \int_0^{\delta_f} |T_s| d\delta \tag{22}$$

and $E_r$ is the required energy to morph the FishBAC active camber structure,

$$E_r = \int_0^{\delta_f} |T_f| d\delta \tag{23}$$

Finally, the nonlinear programming solver *fmincon* in the MATLAB Global Optimization Toolbox was used to optimise the objective function. The resulting optimised parameters are shown in Table 1.

The optimised parameters of the spiral pulley obtained here are theoretical, and only consider the mathematical description of the curve. It is considered here that the torque requirement is a key relationship between these two systems, so the strength of the structures should be considered. For example, the key job of the spiral pulley is transferring different torques here, but the spiral pulley has to support a large force from the both sides of the cordage. Therefore, the thickness of the spiral pulley should be carefully calculated to fabricate a practical spiral pulley for morphing. In addition, in order to remove the influence caused by other factors, such as friction, it is important to carefully mount and align each part of this mechanism.

**TABLE 1**. Optimised parameters for spiral pulley optimisation.

| Parameter | Lower bound | Upper bound | Optimized value | Units |
|---|---|---|---|---|
| Initial radius, $r_0$ | -30/1000 | 10/1000 | -0.0224 | m |
| Pre-exponent term, $k_2$ | -0.001 | 0.020 | 0.0154 | - |
| Exponent term, $k_2$ | 0 | 1 | 0.2135 | - |
| Initial pulley rotation angle, $\delta_0$ | $-50\pi/180$ | $50\pi/180$ | $-12\pi/180$ | rad |
| Drive spring extension, $L_0$ | -0.05 | 0.4 | 0.3254 | m |
| Drive spring rate, $K$ | 100 | 1400 | 766.1927 | N/m |
| Gear ratio, $G$ | 1 | 6 | 4.3309 | - |
| $x_{off}$ | -0.1 | 0.1 | -0.0005 | m |
| $y_{off}$ | -0.05 | 0.10 | 0.0268 | m |

## Simulation results and discussion

With the optimised parameters obtained above, the spiral pulley negative stiffness mechanism can be investigated to determine the effectiveness of an energy balancing system with the positive stiffness FishBAC morphing structure. Figure 7 shows that the evolution of torque with rotation for the spring and the FishBAC and the net torque of the whole system. The torque provided by the spiral pulley negative mechanism matches the torque required closely, and the maximum torque required by the additional actuator is less than 2.5 Nm. We can therefore conclude that the performance predicted for the optimised spiral pulley profile is satisfactory and matches the linearised torque requirements well.

The mechanical energy can be calculated by integrating the torque required to morph the FishBAC, as shown in Fig. 8. By comparing the energy required with and without the negative stiffness mechanism, it shows that the negative stiffness mechanism has a strong ability to passively balance the required actuation energy. Figure 8 shows that the predicted energy reduction is almost 99%, with the energy required reduced from 11.2 J to 0.125 J, which is the contribution of the energy provided by the spiral pulley negative stiffness mechanism.

Figure 9 shows the force available from the spring along with the moment arm provided by the spiral pulley. It can be seen that while the force available from the spring decreases with rotation (16%), the magnitude of the moment arm increases faster (1100%). This is due to the spiral pulley changing its radius when the rotation angle increases, so that the total balancing torque could be produced. In addition, Fig. 9 shows that

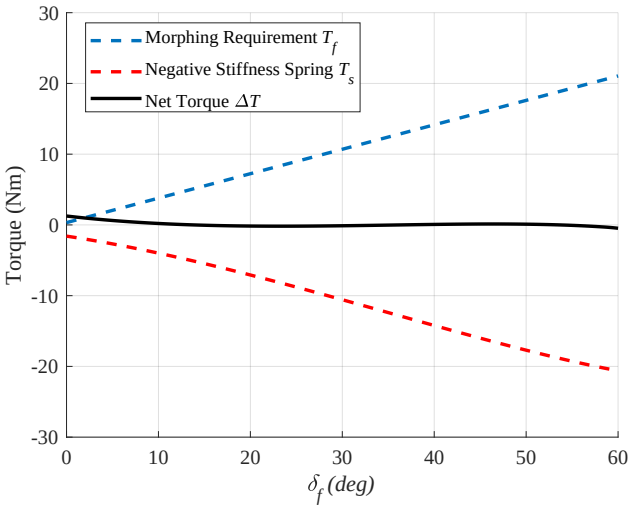


**FIGURE 7**. Predicted torque with the optimised spiral pulley.

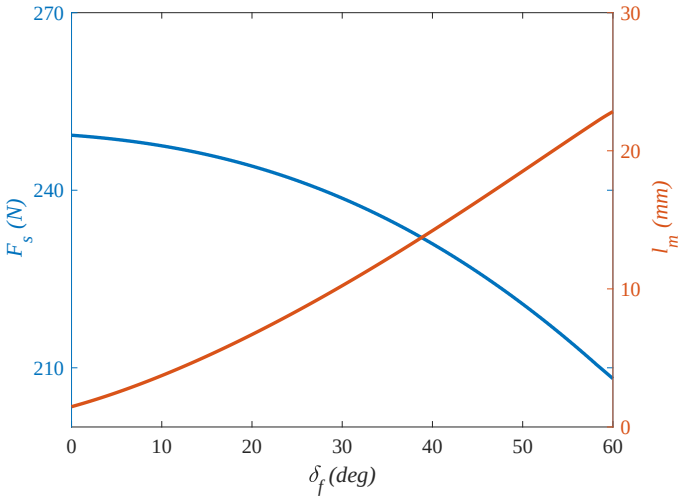


**FIGURE 9**. Evolution of drive spring force with moment arm details.

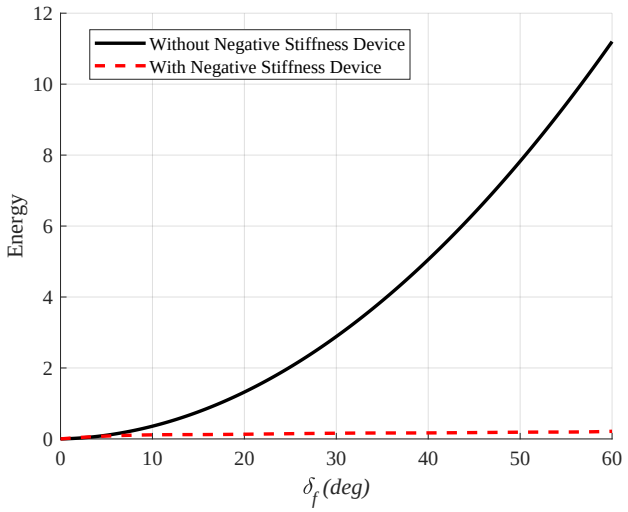


**FIGURE 8**. Comparison of predicted energy required with and without negative stiffness mechanism.

the spring is always extended, which means that only part of the initial extension length is released and the spring will be still extended after actuation. This strategy can avoid a problem in practical application, which is that the initial tension of commercial tension springs can be neglected.

The objective energy conversion efficiency curve plotted in Fig. 10 shows that the optimised configuration of the spiral pulley provides a significantly improved energy efficiency. Moreover, it also shows that the bigger the angle of rotation is, the less energy is needed.

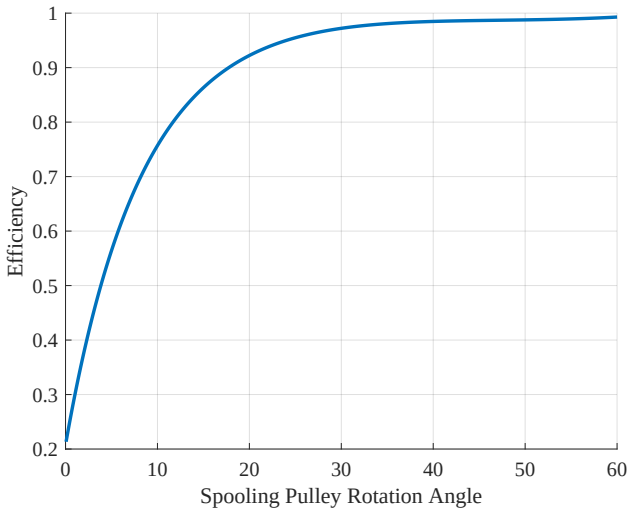


**FIGURE 10**. Evolution of efficiency with rotation.

Based on the investigation of this study, it can be seen that the spiral pulley negative stiffness mechanism provides a significant contribution to balance the positive stiffness system (FishBAC). High energy conversion efficiency can be provided by the prearranged extension spring and a smaller actuator can be used in the whole system.

## Experimental validation

Based on the previous analysis of the spring-drive spiral spooling pulley negative mechanism, an experiment is employed to validate this concept. The spiral pulley was built together with the constant radius pulley, which were 3D printed. Figure 11 shows the pulley, and the radius of the regular pulley is fixed with $R = 13$ mm. The pulleys were mounted onto a central shaft and supported by two bearings. Then, the target drive spring stiffness of 766 N/m was taken from the optimisation results (Table 1), and a commercially available spring with the closest available stiffness was sourced, resulting in an actual drive spring stiffness of 770 N/m (Ashfield Spring Ltd; part number S.74).

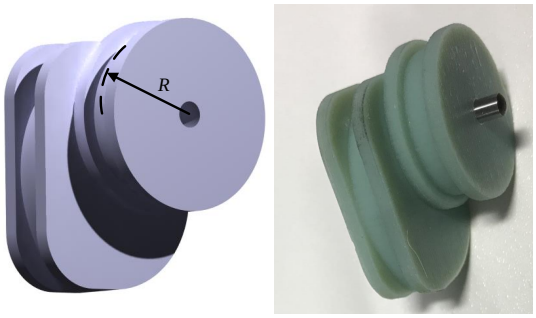


**FIGURE 11**. The experimental spiral pulley.

Figure 12 shows the assembled experimental test rig, which was built on extruded aluminium modular framing. The performance of the spiral pulley system was measured on a Zwick universal load test machine, which provided prescribed displacements and measured the input force. The aluminium structure is first clamped on the test machine. One high-strength spectra fibre cord is connected to the spring and the spiral pulley and another cord is connected between the constant radius pulley and the crosshead of the test machine, as shown in Fig. 12. The test machine stretches the cordage that wraps onto the regular pulley to test the effect of the spiral pulley. The corresponding predicted force required from the analysis for a directly driven shaft was solved by dividing the predicted torque by the known radius of the constant radius pulley and this is compared to the measured force. The friction of the device is neglected in the predictions and the angle is measured by dividing the measured displacement by the known radius of the regular pulley.

The experimentally measured force is now compared with the prediction from the analysis. Figure 13 shows the experimentally measured and analytically predicted evolution of the force for the device. The torque is maximum (0.4 Nm) in the initial state and the torque decreases with increasing displacement until the minimum (0.1 Nm) is obtained. The discrepancy between the experimental result and the analytical result is because of the

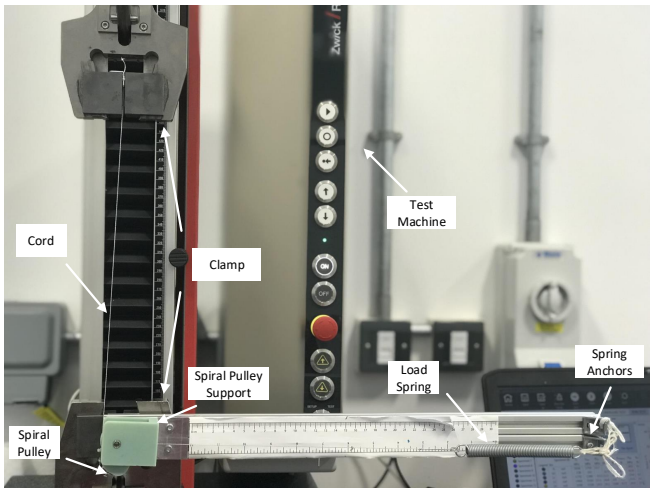


**FIGURE 12**. Photograph of the testing apparatus.

friction. In addition, Figure 12 shows that the cordage which connects the spring and spiral pulley passes through a location hole on the spiral pulley support, which can cause a friction force following the rotation of spiral pulley. But in general, the trend of the negative system is satisfied between the experimental and the analytical result. Therefore, it can be easily understood that if the spiral pulley is initially located at 0° with an optimised extension spring, increasing torque could be obtained due to the profile of the spiral pulley. The results show that the spiral pulley negative stiffness device allows for the drastic reduction in actuation requirement.

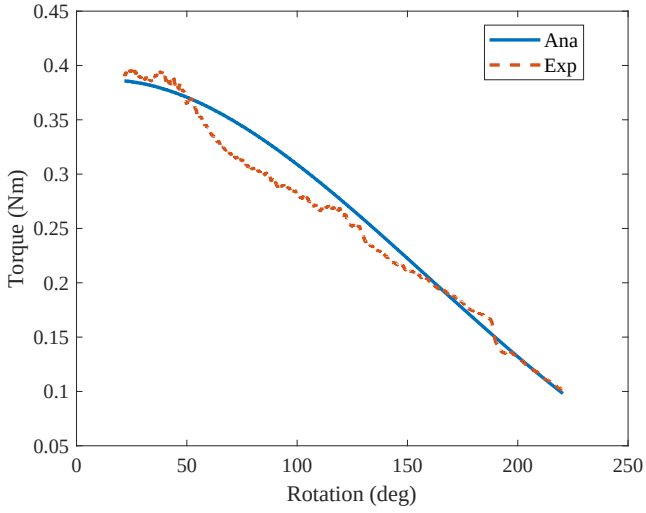


**FIGURE 13**. Comparison of experimental and analytical torque.

## Conclusion

A new concept for using a spiral pulley negative stiffness mechanism for morphing aircraft actuation has been presented. A spiral pulley negative stiffness mechanism was first proposed as the negative stiffness system by using a pre-tensioned spring. The kinematics of the spiral pulley was introduced and the method to convert the positive stiffness spring into a negative stiffness system was investigated. Then, an energy conversion efficiency function was introduced to provide a basis for evaluation and also act as the objective function to optimise the geometry of the spiral pulley simultaneously. The optimised spiral pulley was shown to be able to generate torque that matches the required torque of the FishBAC closely. Thus a significant contribution can be provided by the negative stiffness mechanism to balance the positive stiffness system. Experimental results proved the ability of the spiral pulley negative stiffness device to reduce the torque required by applying the pre-stored energy. Further experiments will be performed to link the negative spiral pulley system to the morphing aerofoil as an energy balancing system to reduce the actuation load. While the example used in this paper is relatively simple, it provides insight into the low energy actuation design problem, both in the field of morphing aircraft and other fields.

## ACKNOWLEDGMENT

This research leading to these results has received funding from the European Commission under the European Unions Horizon 2020 Framework Programme Shape Adaptive Blades for Rotorcraft Efficiency grant agreement 723491.

## REFERENCES

[1] Barbarino, S., Bilgen, O., Ajaj, R. M., Friswell, M. I., and Inman, D. J., 2011. "A review of morphing aircraft". *Journal of intelligent material systems and structures,* ***22***(9), pp. 823–877.

[2] Santos, P., Sousa, J., and Gamboa, P., 2017. "Variable-span wing development for improved flight performance". *Journal of Intelligent Material Systems and Structures,* ***28***(8), pp. 961–978.

[3] Shi, R., and Wan, W., 2015. "Analysis of flight dynamics for large-scale morphing aircraft". *Aircraft Engineering and Aerospace Technology: An International Journal,* ***87***(1), pp. 38–44.

[4] Beaverstock, C. S., Fincham, J., Friswell, M. I., Ajaj, R. M., De Breuker, R., and Werter, N., 2014. "Effect of symmetric & asymmetric span morphing on flight dynamics". In AIAA Atmospheric Flight Mechanics Conference, p. 0545.

[5] Namgoong, H., Crossley, W. A., and Lyrintzis, A. S., 2007. "Aerodynamic optimization of a morphing airfoil using energy as an objective". *AIAA journal,* ***45***(9), pp. 2113–2124.

[6] Ohanian, O., David, B., Taylor, S., Kochersberger, K., Probst, T., Gelhausen, P., and Climer, J., 2013. "Piezoelectric morphing versus servo-actuated mav control surfaces, part ii: Flight testing". In 51st AIAA aerospace sciences meeting including the new horizons forum and aerospace exposition, p. 767.

[7] Tawfik, S. A., Dancila, D. S., and Armanios, E., 2011. "Unsymmetric composite laminates morphing via piezoelectric actuators". *Composites Part A: Applied Science and Manufacturing,* ***42***(7), pp. 748–756.

[8] Lee, T., and Chopra, I., 2001. "Design of piezostack-driven trailing-edge flap actuator for helicopter rotors". *Smart Materials and Structures,* ***10***(1), p. 15.

[9] Hall, S. R., and Prechtl, E. F., 1996. "Development of a piezoelectric servoflap for helicopter rotor control". *Smart Materials and Structures,* ***5***(1), p. 26.

[10] Barbarino, S., Flores, E. S., Ajaj, R. M., Dayyani, I., and Friswell, M. I., 2014. "A review on shape memory alloys with applications to morphing aircraft". *Smart Materials and Structures,* ***23***(6), p. 063001.

[11] Calkins, F. T., and Mabe, J. H., 2010. "Shape memory alloy based morphing aerostructures". *Journal of Mechanical Design,* ***132***(11), p. 111012.

[12] Zhang, J., Zhang, C., Hao, L., Nie, R., and Qiu, J., 2017. "Exploiting the instability of smart structure for reconfiguration". *Applied Physics Letters,* ***111***(6), p. 064102.

[13] Zhang, J., and McInnes, C. R., 2017. "Using instability to reconfigure smart structures in a spring-mass model". *Mechanical Systems and Signal Processing,* ***91***, pp. 81–92.

[14] Daynes, S., Nall, S., Weaver, P., Potter, K., Margaris, P., and Mellor, P., 2010. "Bistable composite flap for an airfoil". *Journal of Aircraft,* ***47***(1), pp. 334–338.

[15] Pontecorvo, M. E., Barbarino, S., Murray, G. J., and Gandhi, F. S., 2013. "Bistable arches for morphing applications". *Journal of Intelligent Material Systems and Structures,* ***24***(3), pp. 274–286.

[16] Karnopp, D., 1995. "Active and semi-active vibration isolation". *Journal of Mechanical Design,* ***117***(B), pp. 177–185.

[17] Churchill, C. B., Shahan, D. W., Smith, S. P., Keefe, A. C., and McKnight, G. P., 2016. "Dynamically variable negative stiffness structures". *Science advances,* ***2***(2), p. e1500778.

[18] Barents, R., Schenk, M., van Dorsser, W. D., Wisse, B. M., and Herder, J. L., 2011. "Spring-to-spring balancing as energy-free adjustment method in gravity equilibrators". *Journal of Mechanical Design,* ***133***(6), p. 061010.

[19] Schenk, M., and Guest, S. D., 2014. "On zero stiffness". *Proceedings of the Institution of Mechanical Engineers, Part C: Journal of Mechanical Engineering Science,* ***228***(10), pp. 1701–1714.

[20] Ostler, J., and Zwick, K., 1939. Power equalizing device, Oct. 31. US Patent 2,178,122.

[21] Woods, B. K., Friswell, M. I., and Wereley, N. M., 2014. "Advanced kinematic tailoring for morphing aircraft actuation". *AIAA Journal,* ***52***(4), pp. 788–798.

[22] Woods, B. K., and Friswell, M. I., 2016. "Spiral pulley negative stiffness mechanism for passive energy balancing". *Journal of Intelligent Material Systems and Structures,* ***27***(12), pp. 1673–1686.

[23] Woods, B. K., Bilgen, O., and Friswell, M. I., 2014. "Wind tunnel testing of the fish bone active camber morphing concept". *Journal of Intelligent Material Systems and Structures,* ***25***(7), pp. 772–785.

[24] Woods, B. K., Dayyani, I., and Friswell, M. I., 2014. "Fluid/structure-interaction analysis of the fish-bone-active-camber morphing concept". *Journal of Aircraft,* ***52***(1), pp. 307–319.

[25] Woods, B. K., and Friswell, M. I., 2013. "Fluid-structure interaction analysis of the fish bone active camber mechanism". In 54th AIAA/ASME/ASCE/AHS/ASC Structures, Structural Dynamics, and Materials Conference, p. 1908.